AIP | Applied Physics Letters

Spin and phonon anomalies in epitaxial self-assembled CoFe2O4-BaTiO3 multiferroic nanostructures

C. Y. Tsai, H. M. Cheng, H. R. Chen, K. F. Huang, L. N. Tsai, Y. H. Chu, C. H. Lai, and W. F. Hsieh

Citation: Applied Physics Letters **104**, 252905 (2014); doi: 10.1063/1.4885497
View online: http://dx.doi.org/10.1063/1.4885497
View Table of Contents: http://scitation.aip.org/content/aip/journal/apl/104/25?ver=pdfcov
Published by the AIP Publishing

Spin and phonon anomalies in epitaxial self-assembled $CoFe_2O_4$-$BaTiO_3$ multiferroic nanostructures

C. Y. Tsai,[1] H. M. Cheng,[2] H. R. Chen,[1] K. F. Huang,[3] L. N. Tsai,[2] Y. H. Chu,[4] C. H. Lai,[3] and W. F. Hsieh[1,a)]

[1]*Department of Photonics and Institute of Electro-Optical Engineering, National Chiao Tung University, 1001 Ta Hsueh Rd., Hsinchu 300, Taiwan*
[2]*Material and Chemical Research Laboratories, Industrial Technology Research Institute, Hsinchu 310, Taiwan*
[3]*Department of Materials Science and Engineering, National Tsing Hua University, Hsinchu 31013, Taiwan*
[4]*Department of Materials Science and Engineering, National Chiao Tung University, Hsinchu 31040, Taiwan*

(Received 30 April 2014; accepted 13 June 2014; published online 26 June 2014)

Temperature dependent magnetic and phonon anomalies in epitaxial self-assembled $CoFe_2O_4$ (CFO) rods embedded in $BaTiO_3$ (BTO) matrix nanostructures were investigated. The temperature dependence of A_1(2TO) phonon frequency of BTO indicates that the BTO matrix experiences structural transformations. The lattice strain produced during the structural transformations drives spin reorientation in CFO rods, resulting in anomalous changes of magnetization. Through correlating the phonon anomalies with the increase of in-plane spin ordering, we show the spin-phonon coupling induces the softening of A_{1g} and A_1(2TO) phonons. It suggests that spin strongly couples with lattice strain and phonons in this nanostructure. © *2014 AIP Publishing LLC*. [http://dx.doi.org/10.1063/1.4885497]

Multiferroic materials simultaneously displaying ferroelectric and ferromagnetic materials have attracted research interests for the coupling between magnetic and electric orders.[1] Recently, much effort has been carried out to realize the stress-mediated coupling in multiferroic materials by applying the external electric fields[2–5] or magnetic fields[6,7] to generate large strain for manipulating the magnetic (or ferroelectric) properties. Because ferroelectric materials undergoing the structural transitions at their Curie temperatures can produce large strain to rotate the magnetic domains, temperature could be a new parameter to modify the interfacial coupling.[8–10] Particularly, the variations of the magnetic domain patterns of ferromagnetic thin films on $BaTiO_3$ (BTO) substrates[8,9,11] have been widely studied by varying the temperature across the ferroelectric transition temperatures. However, for the demand in device miniaturization, the realization of the stress-mediated coupling in nano-scale multiferroic materials becomes interesting and important.

Our previous Raman study on artificial self-assembled nanostructures showed that the magnetostrictive $CoFe_2O_4$ (CFO) rods can generate strain to enhance the polarization of ferroelectric matrix;[7] and X-ray absorption studies revealed an in-plane magnetic field applied on CFO rods can break the local charge symmetry of BTO matrix to create an in-plane polarization.[6] However, how the structural transformations of BTO matrix influence on the magnetic properties of CFO nano-rods remains unknown. In addition, the structure of BTO belongs to rhombohedral below 190 K, orthorhombic from 190 K to 278 K, tetragonal from 278 K to 395 K, and becomes cubic above 395 K.[12] Comparing with the diverse structures of BTO, CFO is ferrimagnetic cubic below 790 K (Ref. 6) that enables one to investigate how the magnetic properties vary with the change of the ferroelectric domains. In this Letter, the temperature dependent magnetic and phonon dynamics were studied in epitaxial CFO-BTO nanostructures across three phase transition temperatures of BTO. We show that not only the structural transition of BTO matrix can induce large strain to alter the magnetic anisotropy of CFO but also the magnetic ordering can renormalize the BTO-A_1(2TO) and CFO-A_{1g} phonon energies via spin-phonon coupling. This indicates a strong coupling between of lattice strain, spin, and phonons.

CFO-BTO films were deposited on (001) oriented $(La_{0.3}Sr_{0.7})(Al_{0.65}Ta_{0.35})O_3$ (LSAT) substrates by using pulsed laser deposition with KrF laser at 900 °C. A composite target of 33% mol $CoFe_2O_4$ and 67% mol $BaTiO_3$ was used. X-ray diffraction (XRD) measurements were conducted using a high-resolution four-circle X-ray diffractometer (HRXRD, Bede D1) with *Cu-kα*$_1$ radiation. Sample topography and magnetic domains were characterized using magnetic force microscopy (MFM, Veeco) operated in tapping mode. Temperature dependent magnetic hysteresis loops were recorded using a Superconducting Quantum Interference Device (SQUID, MPMS-XL). Polarized Raman scattering was excited by the 532 and 325 nm lasers with the power density lower than 1 mW and recorded using a Jobin-Yvon iHR550 spectrometer with a grating of 1800 g/mm equipped with a liquid nitrogen-cooled CCD. The spectra were taken in backscattering geometry with $Z(XX)\bar{Z}$ and $Z(XY)\bar{Z}$ configurations from 80 K to 430 K using a liquid nitrogen-cooled cryostat and a hot stage (THMS600, Linkam), where X, Y, and Z are along [100], [010], and [001] directions, respectively.

XRD patterns in Fig. 1(a) reveal the preferred CFO(004) and BTO(l00) phases orient along the out-of-plane direction as deposited on LSAT substrates. The off-normal XRD scans

a)Author to whom correspondence should be addressed. Electronic mail: wfhsieh@mail.nctu.edu.tw

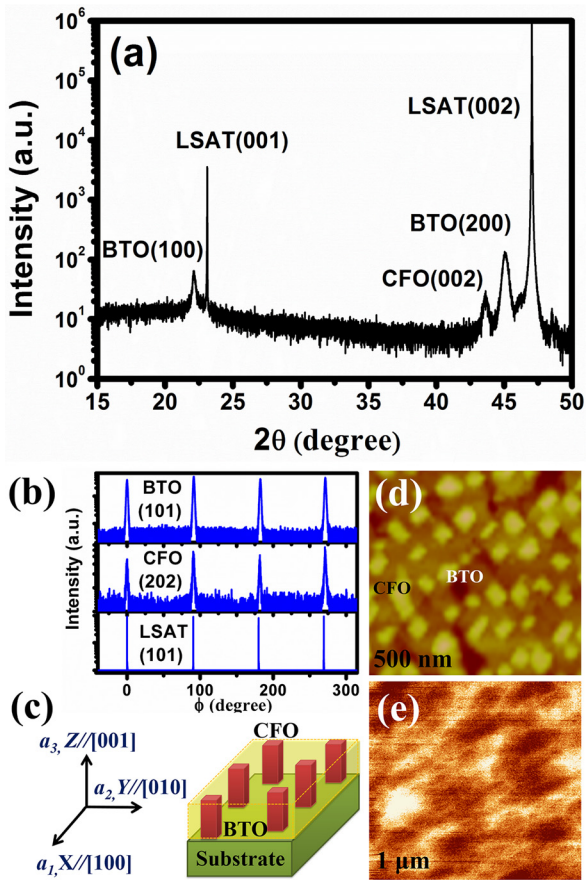

FIG. 1. (a) XRD θ-2θ scan along surface normal and (b) the $\phi-$scan profiles across BTO{202}, CFO{404}, and LSAT{202} off-normal reflections, respectively. (c) The schematic plot of CFO nano-rods embedded in BTO matrix. (d) The sample morphology and (e) the MFM phase image.

across BTO(101), CFO(202), and LSAT(101) reflections in Fig. 1(b) confirm an epitaxial relationship of $(100)[101]_{BTO}$ $||(001)[101]_{CFO}||(001)[101]_{LSAT}$. The calculated lattice constants a_1, a_2, and a_3 are 8.42, 8.41, and 8.30 Å for CFO and 4.04, 4.04, and 4.02 Å for BTO, respectively, where a_1 and a_2 are the in-plane lattice constants and a_3 is the out-of-plane one as indicated in Fig. 1(c). Because the lattice constant of cubic LSAT[13] is 7.736 Å, which is smaller than twice of lattice constants of BTO ($a = b = 3.994$ Å and $c = 4.038$ Å) and that of cubic CFO ($a = b = c = 8.38$ Å), the in-plane tensile stress does not result from strain of substrate. It is found that the lattice constants of CFO are horizontally expanded and vertically compressed when it is embedded in a BTO matrix on $SrTiO_3(001)$ substrate. The out-of-plane compressive strain of -0.94% for CFO rods in this system is close to the strain of -1.1% on $SrTiO_3$ substrate.[1,14] The large lattice strain is attributed to the interplay between BTO and CFO or the smaller thermal expansion coefficients of substrates.[15–18]

The topography image in Fig. 1(d) reveals that the nanostructure contains nano-rods near 50 nm in diameter embedded in a matrix with a distance of 60 nm. Furthermore, the darker and brighter regions of MFM phase image in Fig. 1(e) show the random distribution of the up and down magnetic domains, confirming CFO phase segregates as rods. Therefore, BTO phase is regarded as the matrix. The elongated in-plane lattice parameters of BTO reveal that it is in-plane polarized. The two in-plane lattice constants of BTO are nearly equal, implying the existence of two BTO *a*-domains. This is similar with the two *a*-domains of $PbTiO_3$ (PTO) in CFO-PTO nanostructures.[19]

Figure 2(a) shows the magnetic hysteresis loops at 300 K. The out-of-plane coercive field (H_C) of 0.83 T and the ratio of remanent magnetization (Mr) to saturation magnetization (Ms) of 0.57 are larger than the in-plane ones (less than 0.1 T and 0.05, respectively), revealing a strong magnetic anisotropy with vertical easy axis. We evaluated the shape anisotropy energy density of 3.39×10^5 erg/cm^3 by assuming the 1D model[14] with $E_{shape} = 2\pi(N_X - N_Z)M_S^2$, where the demagnetization factor (N_Z) is 0.040 for a rod aspect ratio of 0.5 and the saturation magnetization (M_S) is 350 emu/cm^3, respectively. The magnetoelastic energy density of 6.98×10^6 erg/cm^3 is comparable large by using a formula of $e = 3\lambda_{001}\sigma_{001}/2 = 3\lambda_{001}Y\varepsilon_{001}/2$,[14] where the magnetostrictive coefficient (λ_{001}), Young's modulus (Y), and the vertical strain (ε_{001}) are -350×10^{-6}, 141.6 GPa, and -0.94%, respectively. The magnetoelastic energy dominates the magnetic anisotropy in consistence with the result of CFO-BTO on $SrTiO_3$.[14] The magnetic anisotropy, however, changes with the temperature, especially around the phase transition temperatures of BTO.[1,11]

In most of the temperature range, the out-of-plane lattice constant a_3 of BTO is shorter than a_1 because it is in-plane polarized. The lattices of BTO and CFO are connected with each other to result in the out-of-plane magnetic anisotropy consisting with the large out-of-plane H_C in Fig. 2(a). However, we observed reduction of out-of-plane H_C and slight increase of in-plane Mr/Ms at 400 K in Fig. 2(b) and the inset therein. It implies that the magnetic preferred orientation gradually deviates away from the out-of-plane direction. Because CFO is a magnetostrictive material, strain can modify its magnetic properties. As BTO structure changes from tetragonal towards cubic, the out-of-plane lattice constant a_3 increases and the in-plane lattice constant a_1 decreases. The in-plane compressive stress of BTO continuously transfers to CFO that reorients the magnetic easy-axis

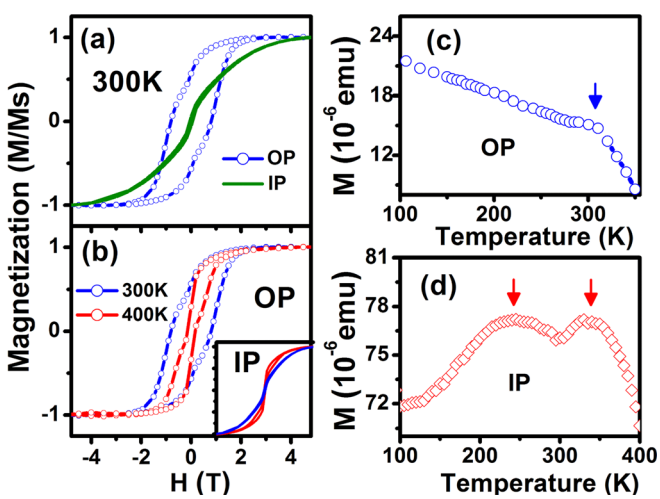

FIG. 2. (a) The magnetic hysteresis loops at 300 K along the out-of-plane (blue circle) and in-plane (green dot) directions. (b) The hysteresis loops at 300 K (blue) and 400 K (red) along out-of-plane direction (circle) and in-plane one (line) in the inset. (c) The temperature dependent out-of-plane magnetization under a magnetic field of 20 Oe and (d) in-plane magnetization under 1000 Oe.

to in-plane direction. It reveals an elastic interaction between these two materials.

The temperature dependent magnetizations (M-T) along out-of-plane and in-plane directions in Figs. 2(c) and 2(d), respectively, reveal the magnetic anomalies. Figure 2(c) shows the gradient of M-T curve that increases the declining trend beyond 310 K. It is known that the magnetization for pure CFO generally smoothly decreases or increases with increasing temperature depending on the field cooling or zero-field cooling process.[20,21] However, the anomalous changed slope beyond 310 K implies that the preferred spin orientation deviates away from the vertical direction because of interfacial coupling with BTO. Furthermore, the similar phenomenon can also be seen in the in-plane M-T curve in Fig. 2(d), which shows continuous increased in-plane magnetization from 300 K to 340 K and then decreases as temperature increases. The spin direction might reorient from the out-of-plane to the in-plane direction driven by the lattice strain, causing the in-plane magnetization to increase, consisting with Figs. 3(b) and 3(c).

Another increase in the in-plane magnetization is found at 250 K.[10] Comparing with M-T curve in Fig. 2(c), the variations of in-plane spin are more sensitive to temperature because of the larger in-plane lattice strain generated by BTO matrix. The transition from orthorhombic to tetragonal structure of BTO at 250 K involves both expansion and compression of in-plane lattice constants.[8] The compressive stress from BTO can drive the spin to orient along the in-plane direction leading to increase the in-plane magnetization at 250 K. After phase transformation, the lattices of BTO continuously increase, which diminishes the magnetic order again and causes magnetization to decrease. The transferred strain from BTO to CFO leads to the electron orbital re-normalizations, which cause the spin to reorient via spin-orbital interaction.[22] It elucidates an efficient coupling between two phases through lattice-orbital-spin interaction. Furthermore, the gradual magnetic changes in this nanostructure differ from the sudden magnetic changes in CFO film deposited on BTO substrate,[11] implying that the complete phase transition of BTO matrix occurs within a broader temperature range.

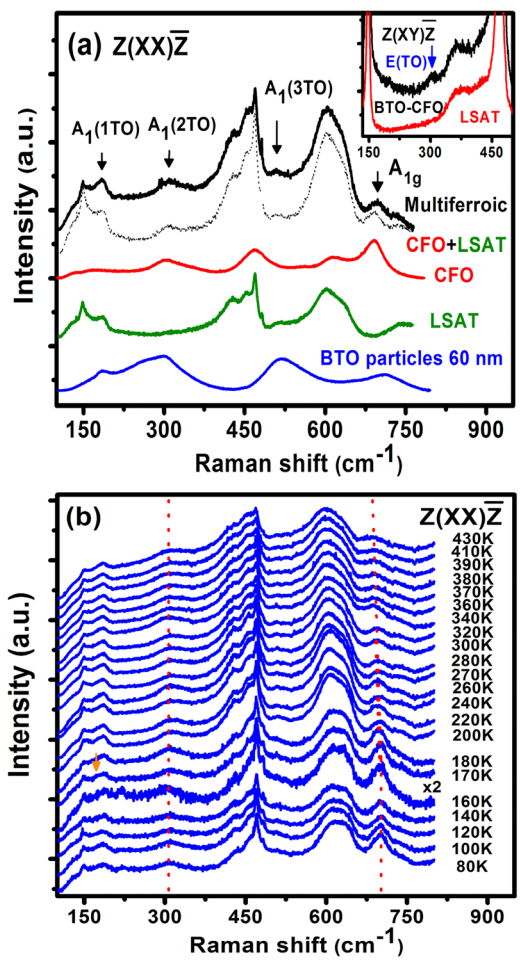

FIG. 3. (a) The polarized Raman spectra of multiferroic nanostructure (black line), BTO nano-particles of 60 nm (blue line), CFO thin films (red line), and LSAT substrate (green line) in parallel $Z(XX)\bar{Z}$ configurations. The black dotted line shows the superposition of CFO and LSAT spectra. The inset shows the crossed $Z(XY)\bar{Z}$ configuration. (b) The polarized Raman spectra in the $Z(XX)\bar{Z}$ configuration from 80 K to 430 K.

The temperature dependent Raman scattering is performed to verify the structural variations. Figure 3(a) shows the Raman spectra for CFO-BTO multiferroic nanostructure, CFO thin film, LSAT substrate, and BTO particles of 60 nm in the $Z(XX)\bar{Z}$ configuration. For cubic CFO with the $Fd\bar{3}m$ symmetry, the E_g and pronounced A_{1g} modes are allowed at 300 cm^{-1} and 700 cm^{-1}, respectively, in the $Z(XX)\bar{Z}$ configuration.[7] According to the P_{4mm} symmetries for an *a*-domain oriented tetragonal BTO, the E(TO) modes are allowed in the $Z(XY)\bar{Z}$ geometry.[23,24] Since E(TO) mode appears at 310 cm^{-1} as shown in the inset of Fig. 3(a), BTO matrix is confirmed as in-plane polarized. Furthermore, three A_1(TO) phonons are allowed at 180, 290, and 520 cm^{-1} in the $Z(XX)\bar{Z}$ configuration.[23] The A_1(2TO) mode is the intense phonon for BTO and shifts towards higher frequency as the grain size decreases.[25] However, it mixes with the CFO-E_g mode at 306 cm^{-1}. Comparing with the ratio of Eg mode intensity to that of A_{1g} mode in pure CFO materials, the intensity ratio in multiferroic nanostructure is much higher, implying that other phonon dominates at 306 cm^{-1}. Because BTO phonon is sensitive to UV laser,[26] this peak is further probed by UV laser, which yields the same frequency of 306 cm^{-1}. Furthermore, the intensity of multiferroic spectrum differs from the superposition of CFO and LSAT spectra, which is shown as the dotted line in Fig. 3(a), especially, at 180 cm^{-1}, 306 cm^{-1}, and 520 cm^{-1}. These frequencies are close to the BTO-A_1(TO) phonon frequencies. Therefore, the phonon mode at 306 cm^{-1} in the $Z(XX)\bar{Z}$ spectrum is dominated by the A_1(2TO) mode. Because of the destructive interference between A_1 phonons, the A_1(1TO) phonon generally appears as an sharp dip at 180 cm^{-1} in the $Y(ZZ)\bar{Y}$ geometry.[23] The interference disappears by using the $Y(XX)\bar{Y}$ geometry.[23] Because BTO is polarized along both a_1 and a_2 directions in this work, the two mixed geometries lead to a peak rather than a dip in spectrum. In addition, the smaller BTO grain size can reduce the interference.[25] We notice the spectrum is characterized by BTO-A_1(2TO) mode at 306 cm^{-1} while CFO-A_{1g} mode dominates at 700 cm^{-1}. The signals from substrate and CFO phonons overlap between 450 and 650 cm^{-1}.

The temperature dependent polarized Raman spectra from 80 K to 430 K are shown in Fig. 3(b) after corrected by

the Bose factor. The fitted phonon frequencies by using Lorentzian functions are plotted in Fig. 4. As shown in the dashed-line in Fig. 4(a), the A_1(2TO) mode frequency of bulk BTO suddenly jumps about 10–20 cm^{-1} at the phase transition temperatures, after that, decreases continuously with increasing temperature, and finally disappears at 395 K.[12,27] The A_1(2TO) phonon frequency of the BTO matrix reveals the similar behaviors, showing anomalous jumps at 160 K, 260 K, and 340 K. It indicates that the phase transformations occur in this nanostructure. Despite the A_1(1TO) mode remains almost the same shape in the whole range, the temperature variation of its phonon frequency basically follows that of A_1(2TO) mode but with smaller frequency jumps, indicating phase transformations. Furthermore, the change from orthorhombic to rhombohedral phase induces two sharp A_1 modes around 171–180 cm^{-1} for bulk BTO.[12,28] For nanostructure, the FWHM of A_1(1TO) mode broadens below 170 K accompanied with the appearance of a small peak near 175 cm^{-1}, which reveals the evidence for rhombohedral phase. According to the fact that the perovskite material has no Raman active modes in paraelectric phase,[29] the appearance of A_1(1TO) and A_1(2TO) phonons up to 430 K indicates that the ferroelectricity of BTO is enhanced. The jump at 340 K could only involve partial cubic phase transition. The origin of enhancing T_C or change of phase transformation temperatures in nanostructure is ascribed to the epitaxial strain from CFO and substrate.[13,24,26,27,30] We notice that in addition to the smaller frequency jumps of 3–10 cm^{-1} than those of bulk BTO, after jumps, the frequency smoothly increases until a peak is reached. Similar with the gradual changes of magnetization in Fig. 2(d), it implies that the transformations are gradual or partial, or other effects are involved.

In Fig. 3(b), the CFO-A_{1g} phonon shows continuously down shifted frequency and broadens as increasing temperatures. Because CFO is absent of phase transformation within 80–430 K, the A_{1g} phonon energy should follow the anharmonic phonon energy, which as proposed by Balkanski,[31,32] is described as $\omega(T)_{anh} = \omega_0 - C(1 + \frac{2}{e^{\hbar\omega/kT}-1})$, where C and ω_0 are adjustable parameters. Figure 4(b) shows the A_{1g} phonon frequency consists well with fitted line except for slight drops at 180 K and 260 K, and strong deviation at 340 K. The phonon anomalies, including the softening of A_{1g}, A_1(1TO), and A_1(2TO) mode frequencies at 340 K, are correlated with the increased in-plane magnetization at 340 K. The spin-spin correlation could renormalize the phonon dynamics via spin-phonon interaction.[33–36] According to a general spin-phonon coupling,[33,34] which is expressed as $\omega = \omega_0 + \lambda\langle S_i \cdot S_j\rangle$, where ω is the phonon frequency under the spin-spin correlation $\langle S_i \cdot S_j\rangle$, λ is the spin-phonon coupling coefficient, and ω_0 is the phonon frequency in absence of spin-spin correlation, the phonon energy reduces because of enhancement of spin ordering.[10] Furthermore, the reduced A_1(2TO) phonon frequency change around 160 K and 250 K compared with that of bulk BTO is ascribed to the increased spin-spin correlation from 135 K to 300 K, which also elucidates the spin-phonon coupling within the spinel-perovskite interfaces. The A_1(2TO) phonon shows strong decreased energy because of spin-phonon coupling, however, the phonon energy of A_{1g} mode reveals slight drops at 180 K and 260 K. At lower temperature, the in-plane spin ordering seems to participate in A_1(2TO) phonon dynamics, which also vibrate along in-plane direction. This indicates the changes of BTO lattices not only reorient the spin-preferred orientation, but also the enhanced in-plane spin ordering, in turn, also perturbs the phonon dynamics either within the spinel region or along the spinel-perovskite interfaces through spin-phonon coupling. It evidences a strong coupling between lattice strain, spin, and phonon in this nanostructure.

In conclusion, the magnetic and phonon dynamics of epitaxial self-assembled CFO-BTO nanostructures are investigated in the temperature range of 80–430 K. Through probing the temperature dependent A_1(2TO) phonon frequency, four structural regions of BTO matrix are elucidated. During phase transformations, the strain transferred from BTO matrix to CFO rods reorients the spin orientation causing magnetic anomalies. Furthermore, the increased spin ordering renormalizes both the A_1(2TO) and A_{1g} phonon energies via spin-phonon coupling. These results suggest the strong coupling of spin with lattice strain and phonons in self-assembled nanostructure.

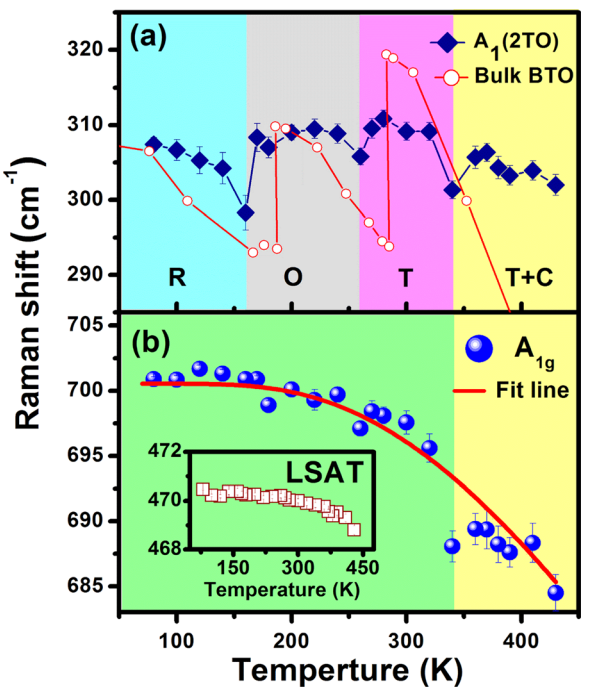

FIG. 4. (a) The temperature dependent A_1(2TO) mode frequency for nanostructure (blue diamond). The red circle shows the phonon frequency of bulk BTO from Perry and Hall.[12] (b) The A_{1g} mode frequency (blue dot) and its anharmonic phonon energy (red line) due to phonon-phonon scattering. The inset shows the phonon position for LSAT substrate, which reveals almost the same frequency.

This work was partially supported by National Science Council of Taiwan under Grant No. NSC-102-2112-M-009-016-MY3.

[1]H. Zheng, J. Wang, S. E. Lofland, Z. Ma, L. Mohaddes-Ardabili, T. Zhao, L. Salamanca-Riba, S. R. Shinde, S. B. Ogale, F. Bai, D. Viehland, Y. Jia, D. G. Schlom, M. Wuttig, A. Roytburd, and R. Ramesh, Science **303**, 661 (2004).
[2]Z. G. Wang, Y. D. Yang, R. Viswan, J. F. Li, and D. Viehland, Appl. Phys. Lett. **99**, 043110 (2011).

[3]N. Jedrecy, H. J. von Bardeleben, V. Badjeck, D. Demaille, D. Stanescu, H. Magnan, and A. Barbier, Phys. Rev. B **88**, 121409 (2013).
[4]T. H. E. Lahtinen, K. J. A. Franke, and S. van Dijken, Sci. Rep. **2**, 258 (2012).
[5]S. Gepraegs, D. Mannix, M. Opel, S. T. B. Goennenwein, and R. Gross, Phys. Rev. B **88**, 054412 (2013).
[6]C. Schmitz-Antoniak, D. Schmitz, P. Borisov, F. M. F. de Groot, S. Stienen, A. Warland, B. Krumme, R. Feyerherm, E. Dudzik, W. Kleemann, and H. Wende, Nat. Commun. **4**, 2051 (2013).
[7]C. Y. Tsai, H. R. Chen, F. C. Chang, H. H. Kuo, H. M. Cheng, W. C. Tsai, Y. H. Chu, C. H. Lai, and W. F. Hsieh, J. Appl. Phys. **115**, 134317 (2014).
[8]T. H. E. Lahtinen and S. van Dijken, Appl. Phys. Lett. **102**, 112406 (2013).
[9]M. C. Pan, S. Hong, J. R. Guest, Y. Z. Liu, and A. Petford-Long, J. Phys. D: Appl. Phys. **46**, 055001 (2013).
[10]A. Ahlawat, S. Satapathy, V. G. Sathe, R. J. Choudhary, and P. K. Gupta, Appl. Phys. Lett. **103**, 252902 (2013).
[11]R. V. Chopdekar and Y. Suzuki, Appl. Phys. Lett. **89**, 182506 (2006).
[12]C. H. Perry and D. B. Hall, Phys. Rev. Lett. **15**, 700 (1965).
[13]B. C. Chakoumakos, D. G. Schlom, M. Urbanik, and J. Luine, J. Appl. Phys. **83**, 1979 (1998).
[14]H. M. Zheng, J. Kreisel, Y. H. Chu, R. Ramesh, and L. Salamanca-Riba, Appl. Phys. Lett. **90**, 113113 (2007).
[15]X. S. Gao, D. H. Bao, B. Birajdar, T. Habisreuther, R. Mattheis, M. A. Schubert, M. Alexe, and D. Hesse, J. Phys. D: Appl. Phys. **42**, 175006 (2009).
[16]M. V. Radhika Rao and A. M. Umarji, Bull. Mater. Sci. **20**, 1023 (1997).
[17]G. Delhaye, C. Merckling, M. El-Kazzi, G. Saint-Girons, M. Gendry, Y. Robach, G. Hollinger, L. Largeau, and G. Patriarche, J. Appl. Phys. **100**, 124109 (2006).
[18]H. Sakowska, M. Swirkowicz, K. Mazur, T. Lukasiewicz, and A. Witek, Cryst. Res. Technol. **36**, 851 (2001).
[19]C. Y. Tsai, H. R. Chen, F. C. Chang, W. C. Tsai, H. M. Cheng, Y. H. Chu, C. H. Lai, and W. F. Hsieh, Appl. Phys. Lett. **102**, 132905 (2013).
[20]T. E. Quickel, V. H. Le, T. Brezesinski, and S. H. Tolbert, Nano Lett. **10**, 2982 (2010).
[21]E. Manova, B. Kunev, D. Paneva, I. Mitov, L. Petrov, C. Estournes, C. D'Orleans, J. L. Rehspringer, and M. Kurmoo, Chem. Mater. **16**, 5689 (2004).
[22]B. D. Cullity and C. D. Graham, *Introduction to Magnetic Materials*, 2nd ed. (Wiley, Hoboken, NJ, 2009).
[23]A. Scalabrin, A. S. Chaves, D. S. Shim, and S. P. S. Porto, Phys. Status Solidi B **79**, 731 (1977).
[24]M. El Marssi, F. Le Marrec, I. A. Lukyanchuk, and M. G. Karkut, J. Appl. Phys. **94**, 3307 (2003).
[25]T. C. Huang, M. T. Wang, H. S. Sheu, and W. F. Hsieh, J. Phys. Condens. Matter **19**, 476212 (2007).
[26]D. A. Tenne, P. Turner, J. D. Schmidt, M. Biegalski, Y. L. Li, L. Q. Chen, A. Soukiassian, S. Trolier-McKinstry, D. G. Schlom, X. X. Xi, D. D. Fong, P. H. Fuoss, J. A. Eastman, G. B. Stephenson, C. Thompson, and S. K. Streiffer, Phys. Rev. Lett. **103**, 177601 (2009).
[27]D. A. Tenne, X. X. Xi, Y. L. Li, L. Q. Chen, A. Soukiassian, M. H. Zhu, A. R. James, J. Lettieri, D. G. Schlom, W. Tian, and X. Q. Pan, Phys. Rev. B **69**, 174101 (2004).
[28]M. Osada, M. Kakihana, S. Wada, T. Noma, and W. S. Cho, Appl. Phys. Lett. **75**, 3393 (1999).
[29]G. Burns and F. H. Dacol, Phys. Rev. B **18**, 5750 (1978).
[30]K. J. Choi, M. Biegalski, Y. L. Li, A. Sharan, J. Schubert, R. Uecker, P. Reiche, Y. B. Chen, X. Q. Pan, V. Gopalan, L. Q. Chen, D. G. Schlom, and C. B. Eom, Science **306**, 1005 (2004).
[31]M. Balkanski, R. F. Wallis, and E. Haro, Phys. Rev. B **28**, 1928 (1983).
[32]A. Ahlawat and V. G. Sathe, J. Raman Spectrosc. **42**, 1087 (2011).
[33]P. K. Pandey, R. J. Choudhary, D. K. Mishra, V. G. Sathe, and D. M. Phase, Appl. Phys. Lett. **102**, 142401 (2013).
[34]Q. C. Sun, C. S. Birkel, J. B. Cao, W. Tremel, and J. L. Musfeldt, ACS Nano **6**, 4876 (2012).
[35]E. Granado, A. Garcia, J. A. Sanjurjo, C. Rettori, and I. Torriani, Phys. Rev. B **60**, 11879 (1999).
[36]R. B. M. Fiho, A. P. Ayala, and C. W. d. A. Paschoal, Appl. Phys. Lett. **102**, 192902 (2013).